

Microstructure and mechanical properties of cubic zirconia (8YSZ)/SiC nanocomposites

Lise Donzel, Steve G. Roberts *

Department of Materials, University of Oxford, Parks Road, Oxford OX1 3PH, UK

Received 29 September 1999; received in revised form 22 March 2000; accepted 28 March 2000

Abstract

The mechanical properties of cubic zirconia (8YSZ)/SiC “nanocomposites” were studied. These properties were found to be strongly dependent on the microstructure and processing conditions. For nanocomposites with SiC particles mostly inside the zirconia grains the bending strength, toughness and hardness were similar to that of monolithic 8YSZ. For nanocomposites with SiC particles located mainly on the grain boundaries, an improvement of the strength and an increase of the toughness were observed. The increase in strength is strongest at room temperature and decreases with rising temperature; the strengths of all materials are identical at $\sim 750^\circ\text{C}$. The higher strength cannot be completely accounted for by the observed increase in toughness, implying a reduced critical flaw size in the stronger material. © 2000 Elsevier Science Ltd. All rights reserved.

Keywords: Mechanical properties; Microstructure-final; Nanocomposites; SiC; SiC-ZrO₂; ZrO₂

1. Introduction

Ceramic nanocomposites are materials in which a reinforcing ceramic phase of nanometric dimensions is added to a ceramic matrix. The interest in such materials has grown after the paper of Niihara,¹ where an increase of strength from 350 MPa to 1 GPa was achieved in Al₂O₃ by incorporating 5 vol.% of SiC nanoparticles. Although the impressive increase of strength reported by Niihara has not been replicated by other groups, most of the subsequent studies showed that reinforcement of Al₂O₃ by SiC particles improves the strength,^{2–5} the wear resistance^{6,7} and creep resistance.^{8,9} Since then many studies have been conducted in this field, mainly on SiC reinforcement of Al₂O₃. Some other systems have also been investigated, for example MgO–SiC,¹⁰ Y₂O₃–SiC,¹¹ ZrO₂–SiC¹² and Si₃N₄–SiC² nanocomposites.

In Al₂O₃–SiC, the improvement of the fracture strength cannot be fully accounted for by increase of the toughness or decrease of the critical flaw sizes. Recently,

a strong effect of machining-induced surface compressive stress on the strength was found.^{4,5} However, when the surface damage is removed by fine polishing, a smaller increase in strength was still observed in the Al₂O₃–SiC with respect to monolithic alumina.⁴ Therefore, the strengthening effect of SiC nanoparticles on Al₂O₃ is not yet clearly understood.

In this study, the effect of SiC nanoparticles on the mechanical properties of cubic zirconia stabilised by 8 mol% yttria, “8YSZ”, was studied. Cubic zirconia was chosen in order to avoid interferences between any effects of SiC additions and the martensitic transformation that occurs in tetragonal zirconia.

2. Experimental procedure

8YSZ/SiC nanocomposite samples containing 5 vol.% of SiC were produced from the following commercial powders: 8YSZ (Dynamic Ceramic Limited, UK) and α -SiC of mean grain size 90 nm (UF 45, Lonza, Germany). The silicon carbide powder was ultrasonically dispersed in distilled water for 20 min and then added to the zirconia powder in an attritor mill with zirconia milling balls. A dispersive agent (Dispex A40, Allied Colloids, UK) was added. After

* Corresponding author. Tel.: +44-1865-273775; fax: +44-1865-272764.

E-mail address: steve.roberts@materials.ox.ac.uk (S.G. Roberts).

milling (2 h, 500 rpm), the slurries were freeze-dried and passed through a 150 μm sieve. The nanocomposites were hot-pressed in BN-coated graphite dies at 1680 and 1710°C for 1 h under a pressure of 20 MPa in nitrogen. Reference zirconia samples were produced in two different ways: (a) by hot-pressing at 1300°C for 1 h under a pressure of 20 MPa in nitrogen; (b) shaped by uniaxial pressing at 40 MPa, further consolidated by cold isostatic pressing (CIP) at 200 MPa and then pressureless sintered at 1400°C for 2 h in air. Final sample dimensions were discs \sim 40 mm diameter, 3.5–4 mm thick.

The density of the samples was measured by Archimedes' method in distilled water. The elastic modulus of the materials was determined using a resonance frequency technique (Grindosonic, Leuven, Belgium).

Microstructural investigations were performed using both scanning electron microscopy (SEM, Hitachi S520) and transmission electron microscopy (TEM, Jeol 200CX). For grain size determination, the samples were polished and then thermally etched for 30 min in air at 1200°C for monolithic zirconias and under vacuum at 1400°C for composite materials. Grain sizes were measured by the linear intercept method. The TEM samples were mechanically ground down to 200 μm thickness, dimpled to 30 μm and then thinned to perforation by an Ar ion beam.

Vickers indentations were made on polished samples (3 μm finish) with a maximum load of 100 N held for 15 s. Ten tests were conducted for each material. The hardness was deduced from the diagonal width ($2a$) of the indentation and the contact load (P) by the following equation:

$$H = \frac{1854.4 \cdot P}{(2a)^2} \quad (1)$$

The toughness (K_c) was calculated from the crack length (c), measured from the indentation centre, using the Anstis formula (half-penny crack):¹³

$$K_c = 0.016 \cdot \left(\frac{E}{H}\right)^{1/2} \left(\frac{P}{c^{3/2}}\right), \quad (2)$$

where E is the elastic modulus.

Hertzian indentations were made on the fine polished materials with a zirconia ball of radius 1 mm using a CK 10 testing machine (Engineering Systems, UK) equipped with an acoustic transducer to detect the initiation of the Hertzian ring crack. It can be shown that there is a minimum indentation load for cracking P_{\min} , below which none of the surface flaws in the Hertzian stress field have a stress intensity greater than K_c .¹⁴ If the sample's surface is stress free, P_{\min} is a function of the sample's toughness and of the Young's modulus and Poisson's ratio of both the sample and the

indenter. If there are compressive residual stresses on the sample's surface, then P_{\min} shifts to a value higher than that for a stress free sample.¹⁵ Experimentally P_{\min} is determined as the lowest fracture load observed in a set of tests statistically large enough (typically 30).

Strength was measured by four-point bending, using beams of size 25.0 \times 2.5 \times 2.0 mm or 15.0 \times 2.5 \times 2.0 mm. The tensile face and the two sides of the specimens were polished down to a finish of 3 μm . The tensile edges were bevelled to prevent edge cracks. The measurements were carried out using an Instron 1362 machine using an adapted Severn Science HTTF-1 furnace for testing up to 1000°C. The outer and inner spans were either 10 and 6 mm, or 22 and 12 mm. The cross-head displacement was 0.5 mm/min. For each material between three and six beams were tested. The nanocomposite beams were tested under Ar in order to avoid oxidation. After the strength tests, the fracture surfaces were observed by SEM.

3. Results

3.1. Microstructure

SEM observation of the polished thermally etched surfaces of fully densified 8YSZ and 8YSZ-5 vol.% SiC samples showed that in all materials the grains are equiaxed. The average grain sizes, d , are given in Table 1. The presence of SiC particles inhibited grain growth and densification. As a result, a much higher temperature is needed to densify the nanocomposites fully, and even at these higher temperatures a fine microstructure is obtained.

In the nanocomposites, TEM observations show that the SiC particles can be found both inside the grains and on the grain boundaries (Fig. 1a and b). There is a clear difference between the microstructures of the two nanocomposite materials studied. In the material hot pressed at 1710°C most grains had internal SiC particles. Some particles and clusters of particles can, however, be found at the boundaries. In contrast, in the sample hot pressed at 1680°C, many grains (more than 50%) are free of internal SiC particles. In this material, the grain growth was too limited to entrap SiC particles in the grains, and most SiC particles are found at the grain boundaries. According to the Niihara classification,¹ the 1710°C material is an "intra/inter" composite and the 1680°C material an "inter" composite.

At some of the grain boundaries and multiple grain junctions an intergranular phase is observed (Fig. 2). This occurs in both nanocomposites. The origin of this phase is not known but could be from powder impurities and/or oxidation of the SiC particles; further detailed compositional studies would be needed to clarify this.

Table 1
Microstructural characteristics and room temperature mechanical properties of the materials tested

	8YSZ–SiC HP 1710°C	8YSZ–SiC HP 1680°C	8YSZ HP 1300°C	8YSZ PS 1400°C
Density (g/cm ³)	5.85 (99.8%)	5.84 (99.7%)	5.98 (99.7%)	5.94 (99.0%)
Grain size (μm)	1.40±0.08	0.61±0.03	1.28±0.26	5.04±0.62
Young modulus (GPa)	227±3	224±3	218±3	209±2
Hardness (GPa)	13.81±0.26	14.98±0.32	15.02±0.45	13.80±0.31
Toughness (MPa√m) _{Vickers}	1.27±0.08	1.95±0.14	1.47±0.21	1.47±0.11
Toughness (MPa√m) _{Hertz}	Not measured	2.1	2.2	Not measured
Strength (MPa)	282±59	555±65	292±63	276±49

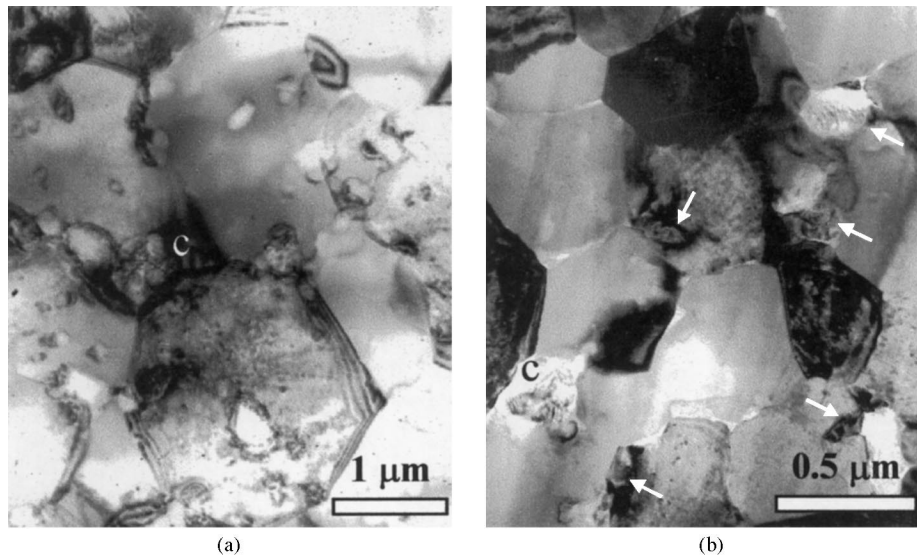


Fig. 1. TEM micrograph of (a) 8YSZ–5 vol.% SiC HP 1710°C and (b) 8YSZ–5 vol.% SiC HP 1680°C. Note the different partition of the SiC particles. Isolated SiC particles are indicated by arrows; clusters of SiC particles are indicated by the letter c.

3.2. Room temperature mechanical behaviour

The room temperature results of the mechanical tests are reported in Table 1. The values of hardness, toughness and strength obtained in this work for 8YSZ (Table 1) are similar to those reported by others for cubic zirconia.^{16,17} The properties of the nanocomposite processed at 1710°C are similar to those of the monolithic materials. Higher toughness and strength are observed for the nanocomposite hot pressed at 1680°C.

SEM observations showed that at room temperature the fracture mode in all materials was mainly transgranular (Fig. 3a and b). This was confirmed by the observation of cracks created by Vickers indentations (Fig. 4a–c). Earlier studies have also found transgranular fracture in cubic zirconia.^{16,17}

Fig. 5 shows the results of Hertzian testing. The minimum fracture loads were used to calculate toughness values; these are reported in Table 1. Results are close to those for Vickers indentation, implying an absence of significant surface residual stresses.

3.3. High temperature strength

Fig. 6 shows four-point bending strength as a function of temperature for hot-pressed and pressureless sintered 8YSZ and for the high strength composite. Fracture strength decreases with increasing temperature in all three materials. At the highest temperature plastic deformation occurred for the pressureless sintered 8YSZ. The strength decrease is more rapid for the high-strength nanocomposite than for the monolithic materials. The fracture mode was mixed at 750°C and mainly intergranular at 1000°C for all materials.

4. Discussion

The results show that the mechanical properties of the 8YSZ/SiC nanocomposites depend strongly on the processing conditions and microstructure. Such an effect was also observed by Bamba et al.⁴ In their fully densified materials, the improvement of the strength becomes

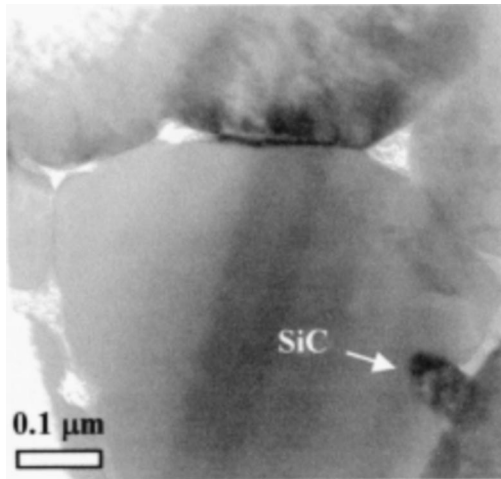


Fig. 2. TEM micrograph showing the intergranular phase found at multiple grain junctions and between grain boundaries (8YSZ–5 vol.% SiC HP 1680°C).

smaller or even disappears with increasing processing temperature. The TEM observations (Fig. 1) show that high strength in the materials tested here is associated with a microstructure consisting of very fine grains with most of the SiC particles located on the grain boundaries, most easily produced at lower temperatures. The improvement in fracture toughness in the nanocomposite material hot pressed at 1680°C in the low temperature regime is not directly related to the fracture mode (transgranular or intergranular) as all materials fractured by transgranular paths at < 500°C.

The Hertzian indentation results (Fig. 5) imply that there are no significant surface residual stresses (e.g. from surface grinding and polishing) in any of the materials tested. In the absence of residual stresses or *R*-curve effects, the fracture strength σ_F of a ceramic is given by

$$\sigma_F = \frac{K_{IC}}{\alpha\sqrt{\pi \cdot c}} \quad (3)$$

where c is the critical (biggest) flaw size, and a is a geometrical factor of about 1. The increase of fracture toughness from 1.47 to 1.95 MPa \sqrt{m} would be expected to increase strength from ~285 to ~380 MPa. If c scales with grain size, a change in grain size from 1.3 to 0.6 μm is consistent with the observed strength of 555 MPa.

The increase of toughness must be related to the presence of SiC particles at the grain boundaries. It is probably a “crack wake” effect, as it is found for cracks of the lengths associated with Vickers indentations (~200 μm), but not those detected by Hertzian indentation (~4 μm). However, it seems not to be due to crack deviation at SiC particles (e.g. by local residual stresses from thermal expansion mismatch), as the SEM observations of Vickers cracks show straight cracks in the high toughness material (Fig. 4c), as for all the other materials. Further, such a mechanism would be expected to be equally effective for intragranular SiC particles, as are found in the nanocomposite hot-pressed at 1700°C — where there is no strength improvement. The strength increase is not related to grain boundary strengthening as fracture is transgranular in monolithic 8YSZ and in the two grades of nanocomposites. Another possible toughening mechanism might be via crack tip shielding by microcracking;¹⁸ however, this is unlikely as this mechanism should scale with the Young’s modulus, and hence would not be expected to drop so rapidly with increasing temperature.

The improvement of the strength of the nanocomposite diminishes rapidly and disappears at 750°C (Fig. 5). This also seems to rule out strengthening related to local residual stresses due to thermal expansion coefficient mismatch between the SiC particles and the ZrO₂, as those should not vanish at so low a temperature. For the same reason softening of the intergranular phase cannot be the origin of the strength decrease. It is interesting to note that this behaviour is different to what is observed in other nanocomposites such as Al₂O₃/SiC, MgO/SiC and Si₃N₄/SiC.¹ In those materi-

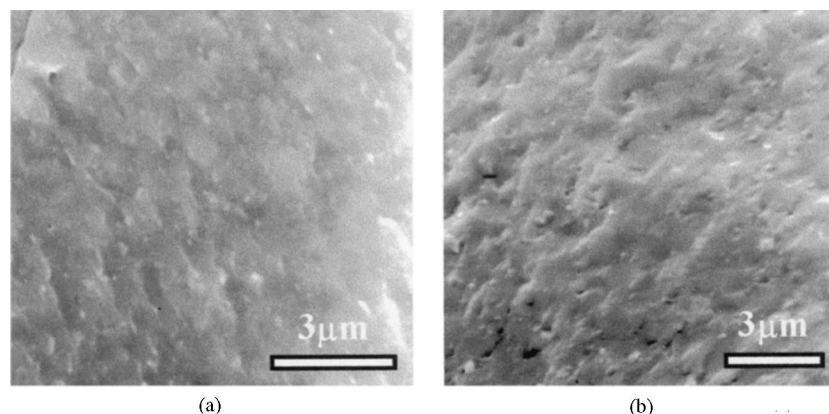


Fig. 3. SEM micrograph of bend specimen fracture surfaces: (a) HP-8YSZ; (b) 8YSZ–5 vol.% SiC HP 1710°C.

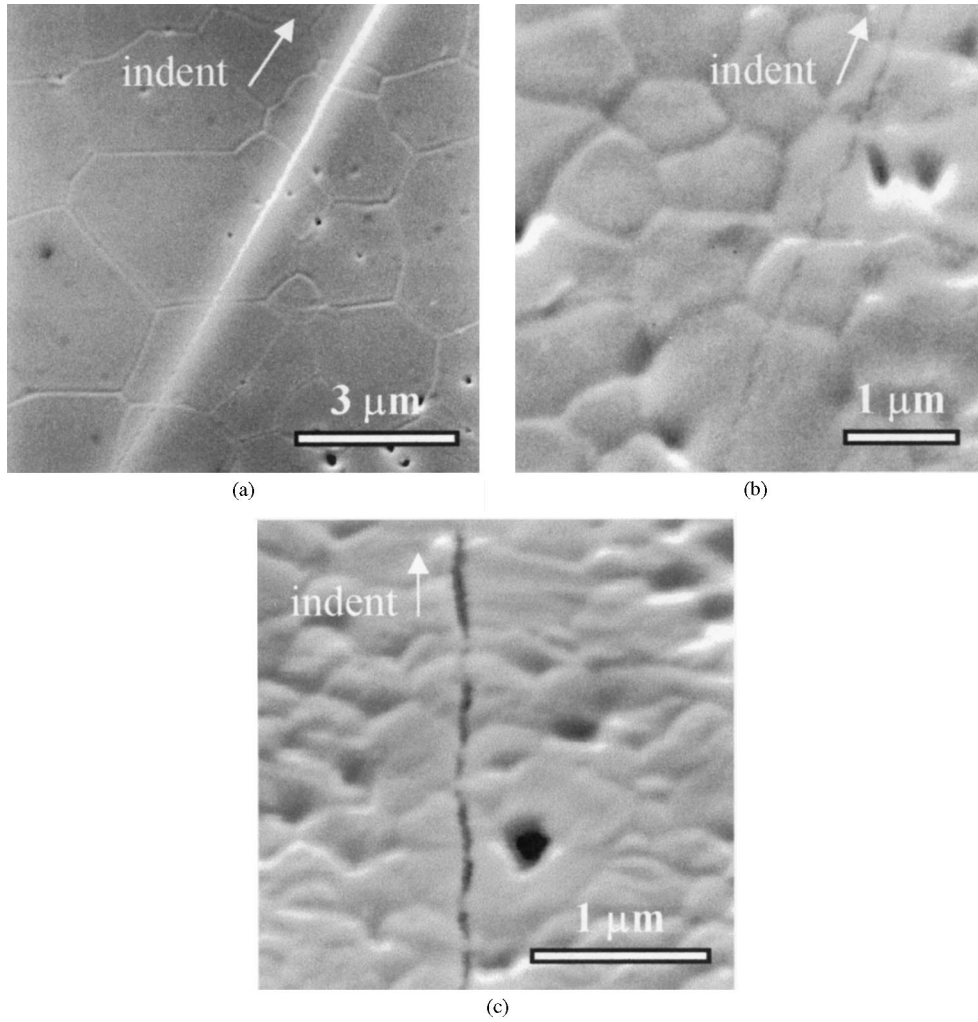


Fig. 4. SEM micrographs of Vickers indentation cracks: (a) PS-8YSZ; (b) 8YSZ–5 vol.% SiC HP 1710°C; (c) 8YSZ–5 vol.% SiC HP 1680°C.

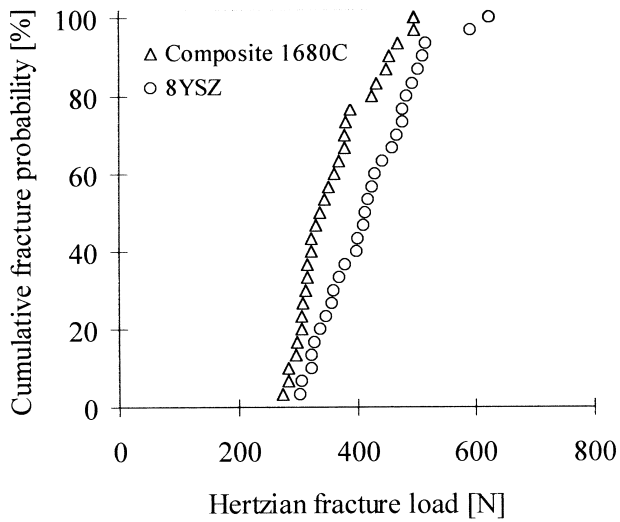


Fig. 5. Cumulative fracture probability as a function of Hertzian indentation fracture load. Surface finish as for the four-point bending beams (3 μm).

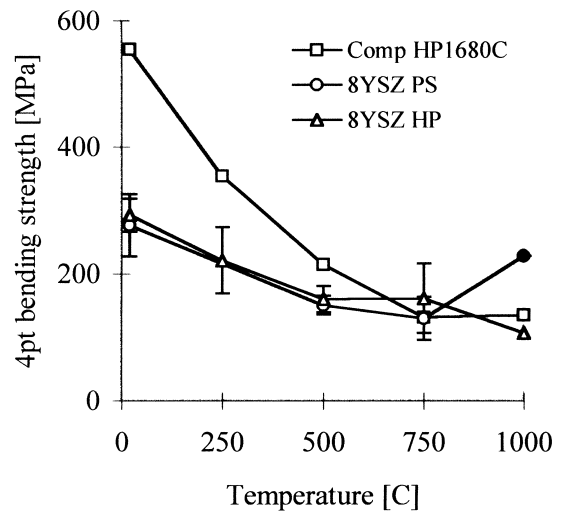


Fig. 6. Four-point bend strength as a function of temperature. Plastic deformation occurred during the 1000°C test for PS-8YSZ (filled symbol).

als the strength improvement is retained up to 1000°C or even above.

5. Conclusions

A high strength 8YSZ/SiC nanocomposite was produced. This improvement in strength could be accounted for by a combination of increased toughness and reduced critical flaw size. The origin of the toughening is not clear, nor is the reason why the improvement in strength decreases so rapidly as a function of the temperature. The present study showed that the microstructure is a critical factor for 8YSZ/SiC nanocomposites. In order to have better mechanical properties than for monolithic 8YSZ, the processing conditions should be such as to lead to limited grain growth with SiC particles located on the grain boundaries rather than in the grains.

Acknowledgements

L.D. would like to thank the Swiss National Science Foundation for funding and B. Derby for initiating this study. H. Wu is thanked for helping with the experiments and fruitful discussions.

References

1. Niihara, K., New design concept of structural ceramics. *J. Ceram. Soc. Jpn.*, 1991, **99**, 974–982.
2. Davidge, R. W., Brook, R. J., Cambier, F., Poorteman, M., Leriche, A., O'Suffivan, D., Hampshire, S. and Kennedy, T., Fabrication, properties and modelling of engineering ceramics reinforced with nanoparticles of silicon carbide. *Br. Ceram. Trans.*, 1997, **96**, 121–127.
3. Perez-Rigueiro, J., Pastor, J. Y., Llorca, J., Elices, M., Miranzo, P. and Moya, J. S., Revisiting the mechanical behavior of alumina/silicon carbide nanocomposites. *Acta Mater.*, 1998, **46**, 5399–5411.
4. Wu, H. Z., Lawrence, C. W., Roberts, S. G. and Derby, B., The strength of Al₂O₃/SiC nanocomposites after grinding and annealing. *Acta Mater.*, 1998, **46**, 3839–3848.
5. Zhao, J., Stearns, L. C., Harmer, M. P., Chan, H. M. and Miller, G. A., Mechanical behavior of alumina–silicon carbide “nanocomposites”. *J. Am. Ceram. Soc.*, 1993, **76**, 503–510.
6. Davidge, R. W., Twigg, P. C. and Riley, F. L., Effect of silicon carbide nano-phase on the wet erosive wear of polycrystalline alumina. *J. Eur. Ceram. Soc.*, 1996, **16**, 799–802.
7. Sternitzke, M., Dupas, E., Twigg, P. and Derby, B., Surface mechanical properties of alumina matrix nanocomposites. *Acta Mater.*, 1997, **45**, 3963–3973.
8. Thompson, A. M., Chan, H. M. and Hamer, M. P., Tensile creep of alumina–silicon carbide “nanocomposites”. *J. Am. Ceram. Soc.*, 1997, **80**, 2221–2228.
9. Nakahira, A., Sekino, T., Suzuki, Y. and Niihara, K., High-temperature creep and deformation behavior of Al₂O₃/SiC nanocomposites. *Ann. Chim. Fr.*, 1993, **18**, 403–408.
10. Choa, Y. H., Nakahira, A. and Niihara, K., Effect of second phase dispersions on microstructure and mechanical properties in MgO/SiC nanocomposites. *Sci. Eng. Comp. Mater.*, 1998, **7**, 249–257.
11. Yoshimura, M., Ohji, Y., Sando, M. and Niihara, K., Microstructure and mechanical properties of Y₂O₃/SiC nanocomposites. *Mater. Res. Innovat.*, 1997, **1**, 16–19.
12. Bamba, N., Choa, Y. H., Sekino, T. and Niihara, K., Microstructure and mechanical properties of yttria stabilized zirconia/silicon carbide nanocomposites. *J. Eur. Ceram. Soc.*, 1998, **18**, 693–699.
13. Anstis, G. R., Chantikul, P., Lawn, B. R. and Marshall, D. B., A critical evaluation of indentation techniques for measuring fracture toughness. *J. Am. Ceram. Soc.*, 1981, **64**, 533–543.
14. Warren, P. D., Determining the fracture toughness of brittle materials by Hertzian indentation. *J. Eur. Ceram. Soc.*, 1995, **15**, 201–207.
15. Roberts, S. G., Lawrence, C. W., Bisrat, Y., Warren, P. D. and Hills, D. A., Determination of surface residual stresses in brittle materials by Hertzian indentation: theory and experiment. *J. Am. Ceram. Soc.*, 1999, **82**, 1809–1816.
16. Navarro, L. M., Recio, P., Jurado, J. P. and Duran, P., Preparation and properties evaluation of zirconia-based/Al₂O₃ composites as electrolytes for solid oxide fuel cell systems. *J. Mater. Sci.*, 1995, **30**, 1949–1960.
17. Cutler, R. A., Reynolds, J. R. and Jones, A., Sintering and characterization of polycrystalline monoclinic, tetragonal and cubic zirconia. *J. Am. Ceram. Soc.*, 1992, **75**, 2173–2183.
18. Hutchinson, J. W., Crack tip shielding by micro-cracking in brittle solids. *Acta Metall.*, 1987, **35**, 1605–1619.